

Astrometric and photometric initial mass functions from the UKIDSS Galactic Clusters Survey: IV Upper Sco ^{*}

N. Lodieu^{1,2†}

¹*Instituto de Astrofísica de Canarias (IAC), Vía Láctea s/n, E-38205 La Laguna, Tenerife, Spain*

²*Departamento de Astrofísica, Universidad de La Laguna (ULL), E-38205 La Laguna, Tenerife, Spain*

Accepted 11 June 2021. Received 11 June 2021; in original form 11 June 2021

ABSTRACT

We present the results of a proper motion wide-field near-infrared survey of the entire Upper Sco (USco) association (~ 160 square degrees) released as part of the UKIRT Infrared Deep Sky (UKIDSS) Galactic Clusters Survey (GCS) Data Release 10 (DR10). We have identified a sample of ~ 400 astrometric and photometric member candidates combining proper motions and photometry in five near-infrared passbands and another 286 with *HK* photometry and 2MASS/GCS proper motions. We also provide revised membership for all previously published USco low-mass stars and substellar members based on our selection and identify new candidates, including in regions affected by extinction. We find negligible variability between the two *K*-band epochs, below the 0.06 mag rms level. We estimate an upper limit of 2.2% for wide common proper motions with projected physical separations less than ~ 15000 au. We derive a disk frequency for USco low-mass stars and brown dwarfs between 26 and 37%, in agreement with estimates in IC 348 and σ Ori. We derive the mass function of the association and find it consistent with the (system) mass function of the solar neighbourhood and other clusters surveyed by the GCS in the 0.2–0.03 M_{\odot} mass range. We confirm the possible excess of brown dwarfs in USco.

Key words: Techniques: photometric — stars: low-mass, brown dwarfs; stars: luminosity function, mass function — galaxy: open clusters and associations: individual (Upper Sco) — infrared: stars — methods: observational

1 INTRODUCTION

The knowledge of the number of stars and brown dwarfs as a function of mass in open clusters and star-forming regions is important to address the question of the universality of the initial mass function (Salpeter 1955; Miller & Scalo 1979; Scalo 1986; Kroupa 2002; Chabrier 2003; Kroupa et al. 2011). The advent of large optical and near-infrared detectors has shed light on the properties of low-mass stars and substellar objects in a variety of environments and enabled an in-depth study of the mass function well below the hydrogen-burning limit (see review by Bastian et al. 2010, and references therein). However, many surveys in young regions lack homogeneity in the multi-band photometric coverage and accurate proper motions for brown dwarf members, making interpretation of their mass spectrum sometimes difficult.

The UKIRT Infrared Deep Sky Survey (UKIDSS; Lawrence et al. 2007)¹ is a deep large-scale infrared survey conducted with the UKIRT Wide field CAMera (WFCAM;

Casali et al. 2007) equipped with five infrared filters (*ZYJHK*; Hewett et al. 2006). All data are pipeline-processed at the Cambridge Astronomical Survey Unit Irwin et al. (CASU; 2004, Irwin et al. in preparation)², processed and archived in Edinburgh, and later released to the community through the WFCAM Science Archive (WSA; Hambly et al. 2008)³. One of its components, the Galactic Clusters Survey (hereafter GCS) imaged ~ 1000 square degrees homogeneously in ten star-forming regions and open clusters down to 0.03–0.01 M_{\odot} (depending on the age and distance of each region) to investigate the universality of the initial mass function. In addition to the photometry, the latest releases of the GCS provide proper motions measured from the different epochs, with accuracies of about five per year (mas/yr).

The USco region is part of the nearest OB association to the Sun, Scorpius Centaurus, located at 145 pc (de Bruijne et al. 1997). Its precise age is currently under debate (Song et al. 2012): earlier studies using isochrone fitting and dynamical studies derived an age of 5 ± 2 Myr (Preibisch & Zinnecker 2002) in agreement with deep surveys (Slesnick et al. 2006; Lodieu et al. 2008) but recently challenged by Pecauc et al. (2012) who quoted

^{*} Based on observations made with the United Kingdom Infrared Telescope, operated by the Joint Astronomy Centre on behalf of the U.K. Particle Physics and Astronomy Research Council.

[†] E-mail: nlodieu@iac.es

¹ The survey is described at www.ukidss.org

² The CASU WFCAM webpage is at <http://apm15.ast.cam.ac.uk/wfcam>

³ WSA is accessible at <http://surveys.roe.ac.uk/wsa>

Table 1. Approximate coordinates of the USco regions from the *ZYJHK*–PM sample with and without extinction, the GCS SV, and the *HK*–only coverage (one in 100 source shown; Fig. 1).

Region	R.A.	dec	Area
	deg	deg	deg ²
No Extinction #1	≤ 244.4	any	33.3
No Extinction #2	≥ 244.4	> -22.5	3.3
Extinction #1	244.4–248.0	≤ -27	7.7
Extinction #2	244.0–246.0	-27.0 to -24.5	3.0
Extinction #3	≥ 246.0	-26.0 to -23.5	5.7
SV #1	241.4–244.3	-24.0 to -22.2	5.2
SV #2	241.8–243.7	-22.2 to -21.4	1.5
<i>HK</i> with Extinction	245.0–249.5	-25.6 to -19.0	29.7

11 ± 2 Myr from a spectroscopic study of F stars at optical wavelengths. The association was targeted at multiple wavelengths, starting off in X rays (Walter et al. 1994; Kunkel 1999; Preibisch et al. 1998), but also astrometrically with Hipparcos (de Bruijne et al. 1997; de Zeeuw et al. 1999), and more recently in the optical (Preibisch et al. 2001; Preibisch & Zinnecker 2002; Ardila et al. 2000; Martín et al. 2004; Slesnick et al. 2006) and in the near–infrared (Lodieu et al. 2006, 2007; Dawson et al. 2011; Lodieu et al. 2011; Dawson et al. 2012). Tens of brown dwarfs have now been confirmed spectroscopically as USco members (Martín et al. 2004; Slesnick et al. 2006; Lodieu et al. 2006; Slesnick et al. 2008; Lodieu et al. 2008; Martín et al. 2010; Dawson et al. 2011; Lodieu et al. 2011) and the mass function of this population determined well into the substellar regime (Slesnick et al. 2008; Lodieu et al. 2011). Three independent studies noticed that USco may harbour an excess of brown dwarfs (Preibisch et al. 2001; Lodieu et al. 2007; Slesnick et al. 2008). Five T–type candidates reported by Lodieu et al. (2011) have been rejected as astrometric members of the association (Lodieu et al. 2013, in press).

In this paper we present a photometric and proper motion–based study of ~ 50 square degrees in USco released as part of the UKIDSS GCS DR10 (14 January 2013) along with a revised analysis of the GCS Science Verification (SV) data (6.7 square degrees). This study is complemented by *HK* imaging and proper motion from the 2MASS/GCS cross–match for the remaining area of the association. Our work improves on previous studies by selecting members based on accurate proper motions provided by the GCS down to masses as low as $0.01 M_{\odot}$ and identifying candidates in regions previously unstudied and affected by heavy extinction. In Section 2 we present the photometric and astrometric dataset employed to extract USco member candidates. In Section 3 we review the list of previously published USco members recovered by our analysis and revise their membership. In Section 4 we identify new stellar and substellar member candidates based on five–band photometry and astrometry. In Section 5 we investigate the level of *K*–band variability for USco low–mass stars and brown dwarfs. In Section 7 we derive the cluster luminosity and (system) mass functions and compare it to earlier estimates for this cluster and others, along with that of the field population. This work is in line with our recent studies of the Pleiades (Lodieu et al. 2012), α Per (Lodieu et al. 2012), and Praesepe (Boudreault et al. 2012) clusters.

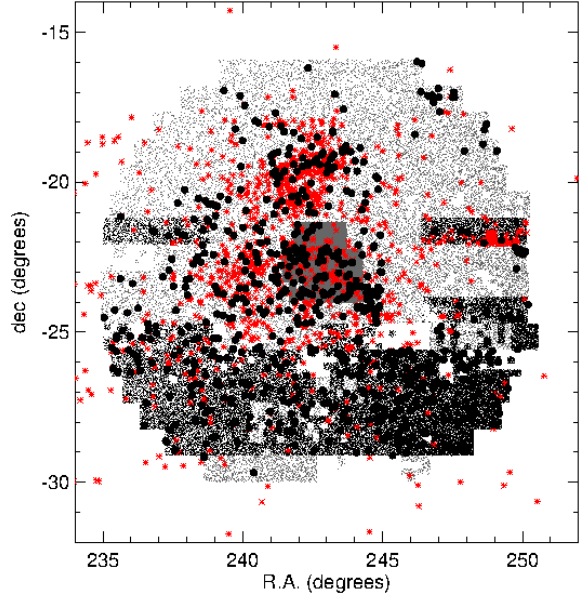


Figure 1. The coverage in USco as released by the UKIDSS GCS DR10: the light grey, dark grey, and black patches indicate the *HK*, SV, and GCS DR10 samples, respectively. The holes are due to frames removed from the GCS release due to quality control issues. Overplotted are member candidates identified in this work (filled black dots) and previously-published sources from the literature (red asterisks).

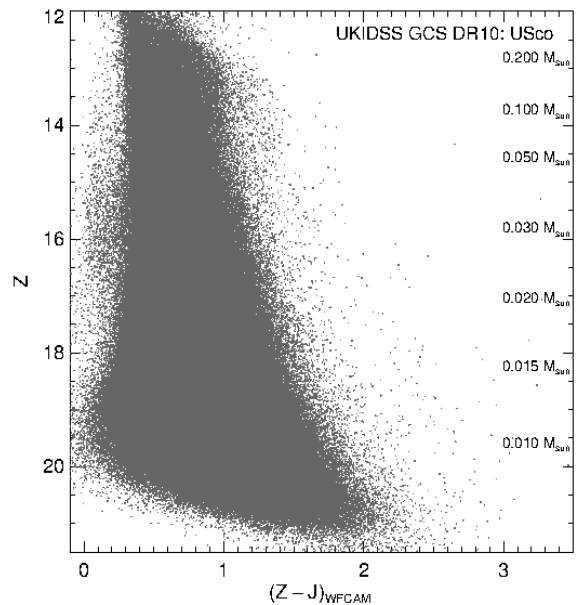


Figure 2. $(Z - J, Z)$ CMD for ~ 50 square degrees in USco extracted from the UKIDSS GCS DR10. The mass scale shown on the right hand side spans ~ 0.2 – $0.08 M_{\odot}$, following the 5–Myr BT–Settl isochrones (Allard et al. 2012).

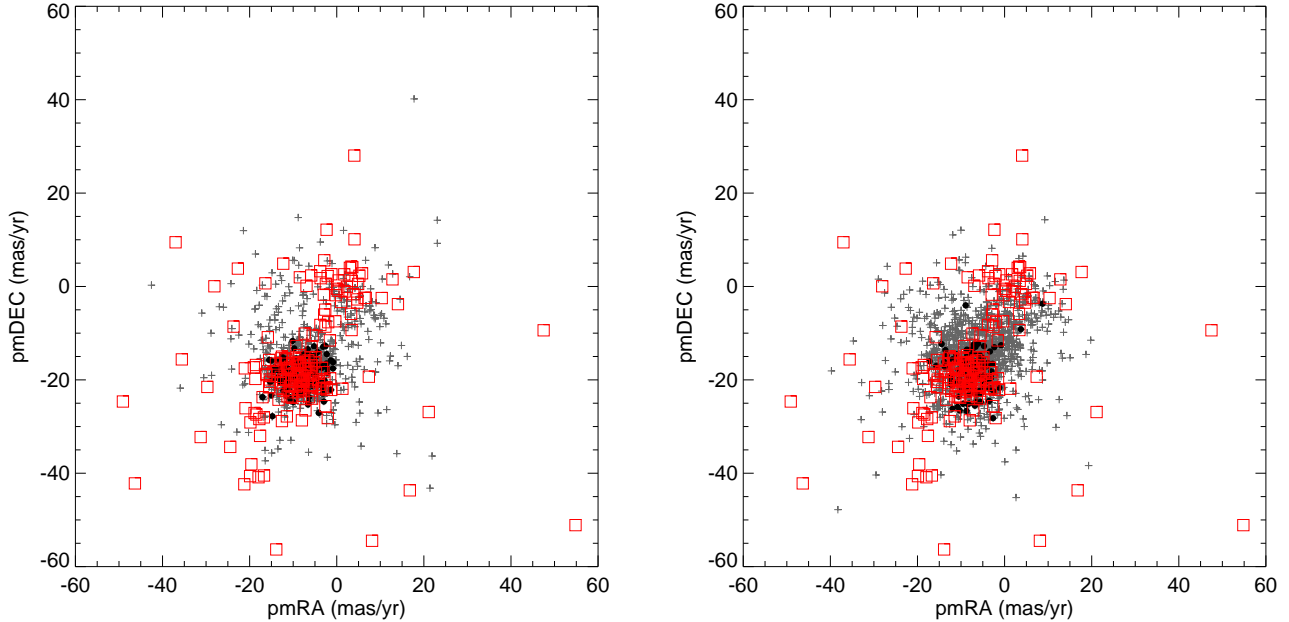


Figure 3. Vector point diagrams showing the proper motions from the GCS alone in right ascension (x-axis) and declination (y-axis) for previously-known member candidates recovered by the GCS DR10 (red open squares) and all point sources after the crude photometric selection made in the $(Z - J, Z)$ colour-magnitude diagram for the $ZYJHK-PM$ sample. Black filled dots are our photometric and astrometric member candidates in USco. *Left:* Vector point diagram for a region without extinction. *Right:* Same diagram for the area of USco affected by reddening.

2 THE SAMPLE

We selected point sources in the full USco region, defined by $RA=230-252$ degrees and declinations between -32 and -16 degrees (Fig. 1). We retrieved the catalogue using a Structure Query Language (SQL) query similar to our earlier studies of the Pleiades (Lodieu et al. 2012), α Per (Lodieu et al. 2012), and Praesepe (Boudreault et al. 2012). Briefly, we selected high quality point sources with JHK photometry, allowing for Z and Y non detections. The query returned a total number of 2,943,321 sources. We refer to this sample as the “ $ZYJHK-PM$ ” sample throughout the paper. Below we distinguish the region free of extinction and the one affected by reddening although we will show that the same photometric and astrometric criteria can be applied to provide a clean sample of member candidates.

Proper motion measurements are available in the WFCAM Science Archive for UKIDSS data releases from DR9 for all the wide/shallow surveys with multiple epoch coverage in each field (i.e. the LAS, GCS and GPS). Details of the procedure are in Collins & Hambly (2012) and summarised in Lodieu et al. (2012) for the purpose of the Pleiades. The typical error bars on the GCS proper motions in USco are 4 mas/yr and 6 mas/yr, down to $Z = 19$ mag and 20 mag, respectively (Fig. 3).

First, we applied a crude photometric selection to work with a subsample of the entire catalogue. We selected all sources located to the right of the line running from $(0.5, 12)$ to $(2.2, 21.5)$ in the $(Z - J, Z)$ colour-magnitude diagram (Fig. 4). We made sure that this line allowed us to recover known spectroscopic members (see Section 3). This sample contains 29,382 sources, divided into 9351 in the region free of extinction and 20,031 in the parts affected by reddening (Fig. 1; Table 1).

The rest of the USco association is not covered with enough epochs to measure proper motions based only on GCS data. This is

the case for the GCS SV (Table 1) and the area covered in HK only. In the case of the GCS SV area, we have $ZYJHK$ photometry and proper motions measured from the 2MASS/GCS cross-match. Lodieu et al. (2007) identified member candidates in this part of the association (although with a slightly smaller area released at that time) and confirmed a large number as spectroscopic members (Lodieu et al. 2011). Dawson et al. (2012) also included this region in their study of the disk properties of USco low-mass and brown dwarfs, as did Riaz et al. (2012). We have 430 sources in the GCS SV region, after applying the crude photometric selection described above.

We added to those samples the full coverage of the GCS DR10, only imaged in the H and K passbands (hereafter the HK sample). We also measured proper motions from the 2MASS/GCS correlation. Our query returned a total of 7,328,848 to which we should remove the GCS SV and GCS DR10 samples as well as the region most affected by reddening (defined by $R.A. = 245-249.5$ degrees and dec between -25.6 and -19 degrees, see Table 1). We applied a crude photometric selection in the $(H - K, H)$ colour-magnitude diagram, keeping only sources to the right of a line running from $(H - K, H) = (0.2, 12)$ to $(0.7, 18)$. We are left with 39,450 sources to investigate astrometrically (Sect. 4.1).

3 CROSS-MATCH WITH PREVIOUS SURVEYS

We compiled a list of USco members published over the past decades by various groups (Preibisch et al. 1998, 2001; Preibisch & Zinnecker 2002; Ardila et al. 2000; Martín et al. 2004; Slesnick et al. 2006; Lodieu et al. 2006, 2007, 2008; Dawson et al. 2011; Lodieu et al. 2011; Dawson et al. 2012; Luhman & Mamajek 2012) to update their membership status with the photometry and astrometry provided by the GCS DR10 (Table 2). This list will

serve as starting point to identify new member candidates in the GCS, estimate the mean (relative) proper motion of USco members, and derive the cluster luminosity and mass functions. We compiled a list of 2079 candidates, reduced to 1566 after removing multiple pairs.

We cross-correlated this list of 1566 known member candidates with the *ZYJHK*–PM catalogue using a matching radius of three arcsec and found 125 sources in common (red open squares in Fig. 3; Table 2). We repeated the same process with the GCS SV and *HK*-only areas, yielding 73 and 651 member candidates in common, respectively (Table 2). The number of known member candidates recovered in GCS DR10 is generally low because most surveys focussed on the northern area with right ascensions between 240 and 245 degrees and declinations above -25° (see list of sources in Luhman & Mamajek 2012). Below we provide a few comments on the recovery rate for the early studies listed in Table 2.

- The samples published by Preibisch et al. (2001) and Preibisch & Zinnecker (2002) lie outside the GCS DR10 and SV areas and very few objects of the X-ray and proper motion catalogues of Preibisch et al. (1998) lie in those regions as well as X-ray and proper motion samples of Preibisch et al. (1998). Most of the members from Preibisch et al. (1998) and Preibisch et al. (2001) are too bright for the UKIDSS GCS and generally saturated because they are brighter than $B = 15.3$ mag and have spectral types earlier than M.

- All candidates identified in the successive GCS releases by Lodieu et al. (2006), Lodieu et al. (2007), Dawson et al. (2011), and Dawson et al. (2012) are recovered by our analysis but the assessment of their membership changes slightly following the improvement on the proper motions from the 2MASS/GCS cross-match to the two GCS epochs. They are covered by the GCS DR10 *ZYJHK*–PM and SV samples.

- The full catalogue of USco members published by Luhman & Mamajek (2012) contains a total of 863 sources, including 381 brighter than $J = 11.5$ mag, which are saturated on the GCS images. Hence, our recovery rate of 405 sources out of $(863 - 381) = 482$ in the GCS is over 80%. Similarly, we recovered 472 sources among the 806 with *HK* photometry, which is over 98% completeness because most of the other objects are saturated in the GCS.

- The recovery of candidates published by the remaining studies is mainly biased due to the lack of overlap between those surveys (red asterisks in Fig. 1) and the *ZYJHK*–PM and GCS SV. Table 2 **demonstrates** that most of the sources published by previous studies are part of the region covered in *H*, *K*. The most incomplete recoveries are due to the bright early-type members in the catalogues of Preibisch et al. (1998), Preibisch et al. (2001), and Luhman & Mamajek (2012) as discussed in the previous bullets.

4 NEW USCO LOW-MASS AND BROWN DWARF MEMBER CANDIDATES

4.1 Astrometric selection

After the original photometric selection and the recovery of known member candidates, we plotted them as red open squares in Fig. 3. We observe two groups of objects, one centered on (0,0) made of field objects, and another one depicting the position of USco. We measured mean (relative) proper motions of -8.6 and -19.6

Table 2. Numbers of USco member candidates recovered in the full GCS database using a matching radius of $3''$ before running our SQL queries (GCS), in the *ZYJHK*–PM sample (DR10), in the SV area (SV), and in the *HK*–only region. Papers dedicated to USco are listed below and ordered by year. References are: Preibisch et al. (1998, X-ray and proper motion samples), Preibisch et al. (2001), Preibisch & Zinnecker (2002), Ardila et al. (2000), Martín et al. (2004), Slesnick et al. (2006), Lodieu et al. (2006), Lodieu et al. (2007), Lodieu et al. (2008), Dawson et al. (2011), Lodieu et al. (2011), Dawson et al. (2012), Luhman & Mamajek (2012). The last column lists the percentage of sources in the original paper recovered in the *ZYJHK*–PM coverage with and without extinction.

Survey reference	GCS	DR10	SV	<i>HK</i>	%
Preibisch1998_Xray	20/78	0/10	0/10	10/55	25.6
Preibisch1998_PM	21/115	2/20	0/1	14/89	18.3
Preibisch2001	0/100	0/0	0/0	7/100	0.0
Preibisch2002	0/166	0/0	0/0	98/166	0.0
Ardila2000	17/20	1/2	0/0	14/20	85.0
Martin2004	10/40	2/6	2/4	36/36	25.0
Slesnick2006	7/38	2/2	2/5	33/34	18.4
Lodieu2006	15/15	15/15	0/0	15/15	100.0
Lodieu2007	129/129	0/0	64/129	97/129	100.0
Slesnick2008	38/145	10/12	16/26	127/140	26.2
Dawson2011	28/28	28/28	0/0	28/28	100.0
Dawson2012	116/116	74/74	35/42	116/116	100.0
Luhman2012	405/863	47/92	65/173	472/806	46.9
Total	186/1566	125/158	73/202	651/1066	11.9

mas/yr in right ascension and declination, respectively, compared to the absolute values of -11 and -25 mas/yr from Hipparcos (de Bruijne et al. 1997; de Zeeuw et al. 1999). We noticed the same effect in the Pleiades (Lodieu et al. 2012), α Per (Lodieu et al. 2012), and Praesepe (Boudreault et al. 2012) because the GCS provides *relative* motions rather than *absolute* motions as in the case of Hipparcos. We applied a 3σ astrometric selection using the error bars for each source from the GCS in both directions, leaving 87 of the 186 known member candidates in the *ZYJHK*–PM sample.

We applied the same 3σ astrometric selection to the full sample of point sources towards USco, both for the sample free of extinction and the one affected by reddening. In the former case, we are left with 700 of the original 9351 sources, and, in the latter, 1357 of the 20,031 objects (grey crosses in Fig. 3). We plot these proper motion member candidates as grey crosses in the colour-magnitude diagrams displayed in Fig. 4. We tested the influence of our choice of the relative proper motion values in right ascension and declination by adding and removing 1 mas/yr in both directions (about 20% of the mean error bars on the proper motions). We found that the numbers of candidates would change by less than 5.4% (677 and 738 candidates in the worst cases compared to 700) and 8.3% (1253 and 1468 compared to 1357) in the case of the *ZYJHK*–PM samples without and with reddening, respectively.

For the remaining areas of the association, we measured the proper motions from the 2MASS/GCS cross-match, whose accuracy is about twice worse than the GCS proper motions (10 mas/yr down to $J = 15.5$ mag). The mean proper motion of known spectroscopic members in the SV area is -8.5 and -19.2 mas/yr in right ascension and declination, respectively. As described above, those values differ from the absolute mean proper motion of USco but we used them for our 2MASS/GCS astrometric selection. We note that these values are very similar to the mean proper motions derived from the two GCS epochs. We are left with 242 sources out of the

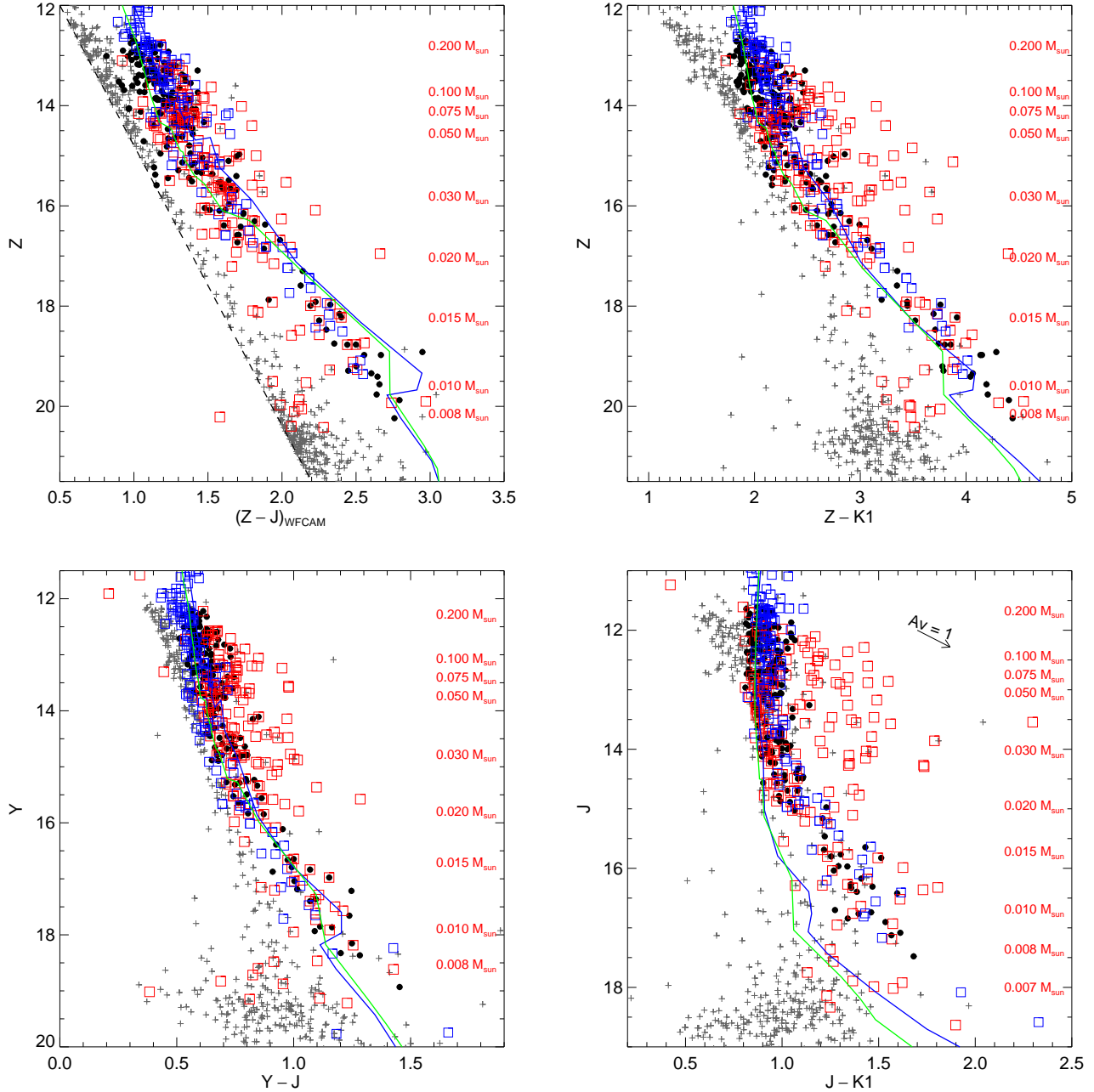


Figure 4. Colour-magnitude diagrams showing the USco member candidates previously reported in the literature (red open squares) and the new ones identified in this work (black dots). Photometric and/or proper motion non-members are highlighted as grey crosses. Known spectroscopic members are overplotted as blue open squares (Lodieu et al. 2011). Overplotted are the 5 and 10 Myr-old BT-Settl isochrones (Allard et al. 2012) shifted at a distance of 145 pc. The mass scale shown on the right hand side of the diagrams spans approximately 0.2–0.008 M_{\odot} , according to the 5 Myr isochrones. The dashed line in the upper left diagram represent our crude photometric selection using a line running from $(Z - J, Z) = (0.5, 12.0)$ to $(2.2, 21.5)$. Upper left: $(Z - J, Z)$; Upper right: $(Z - K, Z)$; Lower left: $(Y - J, Y)$; Lower right: $(J - K, J)$.

430 original photometric candidates in the GCS SV area, after applying a 2σ selection (Table C1). Changing the mean values of the proper motions in each direction by ± 1 mas/yr results in a number of member candidates that differs by less than 3.75%.

For the HK -only area, the situation is worse than for the SV region because we have only two bands available ($H + K$) where the cluster sequence is not so well separated from the field stars along the line of the association as in the $(Z - J, Z)$ colour-

magnitude diagram. Hence, our final HK sample will be significantly more contaminated than the aforementioned samples. First, we applied a conservative photometric selection in the $(H - K, H)$ diagram by considering only point sources to the right of a line running from $(H - K, H) = (0.2, 12)$ to $(0.7, 18)$. After this first step, we are left with 63,520 candidates. Second, we applied a 2σ astrometric selection (i.e. 2×10 mas/yr or 95.4% completeness) in the $H = 12.5$ – 15 mag interval (corresponding to masses ranging from

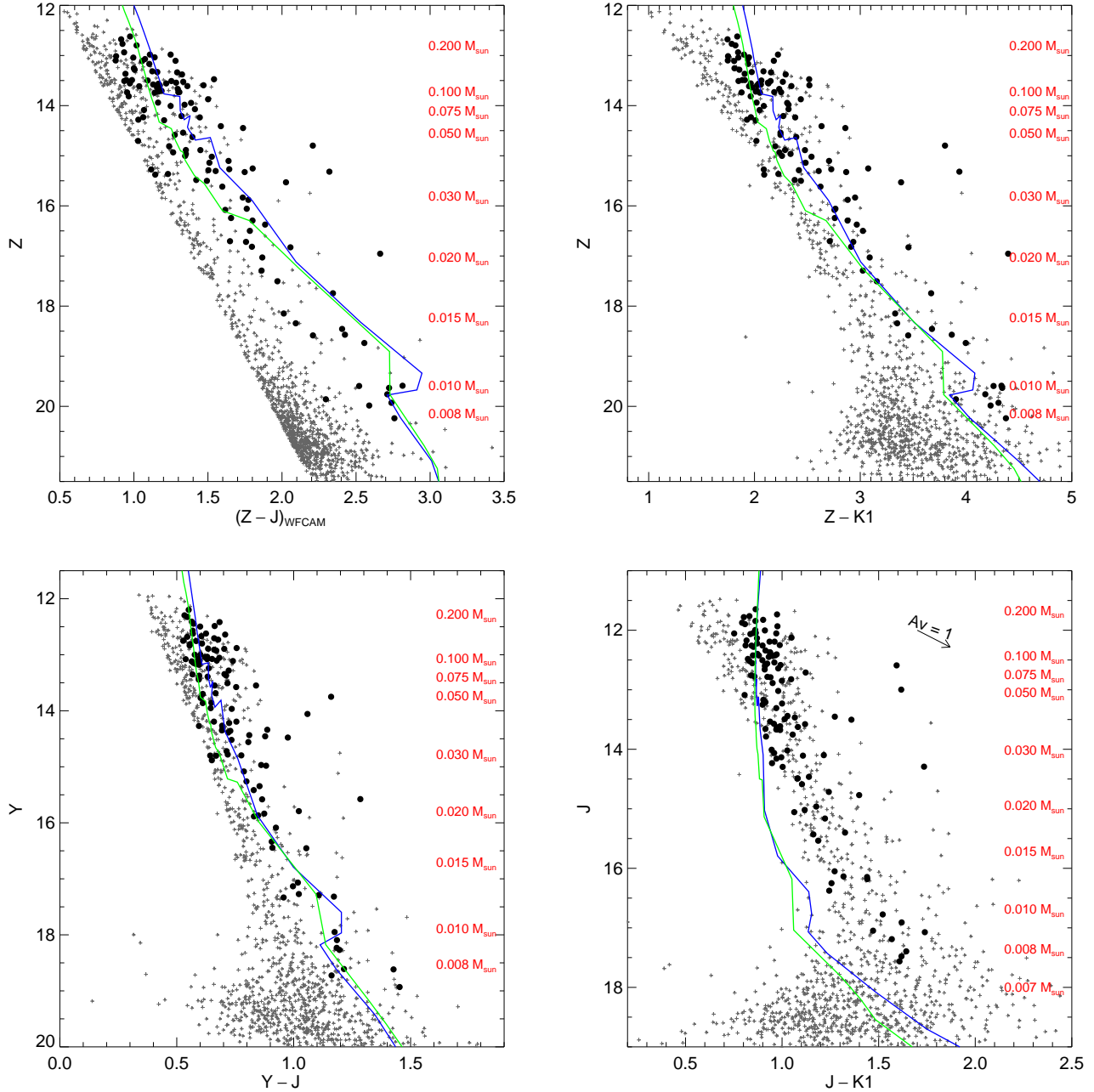


Figure 5. Same as figure 4 but for the region in USco affected by reddening.

0.12–0.175 M_{\odot} to 0.015–0.02 M_{\odot} for ages of 5 and 10 Myr, respectively), yielding 976 candidates. Third, we applied a stricter photometric selection in the $(H - K, H)$ diagram, keeping sources to the right of a line running from (0.31, 12.5) to (0.7, 16.5). This line was chosen to recover all photometric and astrometric candidates from the SV-only and $ZYJHK$ -PM samples. We are left with 286 candidates in the HK region (Fig. 1; Table D1). We tested the influence of our astrometric selection by changing the mean proper motion in RA and dec by ± 1 mas/yr, yielding in the extreme cases 281 and 304 candidates i.e. a difference of 6.3% in the worst case compared to our original choice. The main uncertainty on the number of candidates in the HK -only sample rather comes from the choice of the sigma in the astrometric selection: choosing 2.5σ

(99% completeness) and 3σ (99.9% completeness) would lead to 360 and 412 candidates, respectively.

4.2 Photometric selection

To further refine our list of USco member candidates we applied additional photometric cuts in various colour-magnitude diagrams for the $ZYJHK$ -PM sample, defined as follows:

- $(Z - K, Z) = (1.60, 12.0)$ to $(2.20, 16.0)$
- $(Z - K, Z) = (2.20, 16.0)$ to $(4.00, 20.0)$
- $(Y - J, Y) = (0.40, 12.0)$ to $(0.65, 15.0)$
- $(Y - J, Y) = (0.65, 15.0)$ to $(1.00, 18.0)$

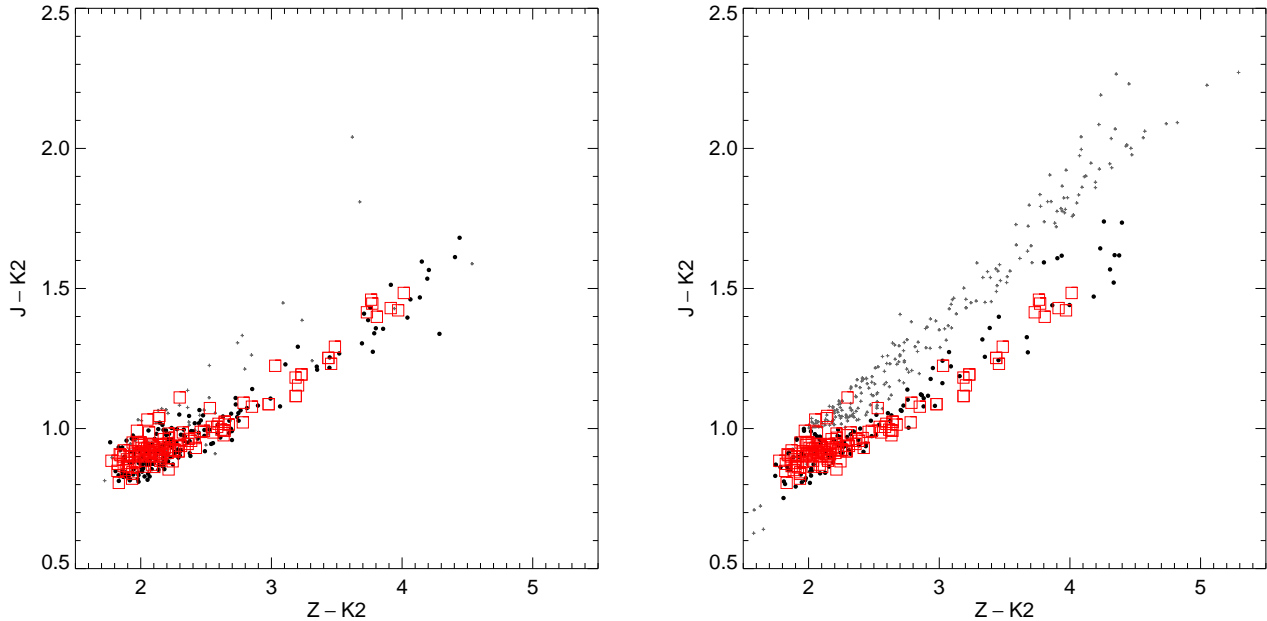


Figure 6. $(Z - K, J - K)$ colour-colour diagram for the photometric and astrometric candidates (grey crosses) in the region free of extinction (left) and the region affected by reddening (right) of the $ZYJHK-PM$ sample. Overplotted as red open squares are known spectroscopic members. USco candidate members identified in our study are plotted as black dots.

- $(J - K, J) = (0.80, 11.5)$ to $(0.80, 14.0)$
- $(J - K, J) = (0.80, 14.0)$ to $(1.40, 18.0)$

The numbers of candidates after the $Z - K$, $Y - J$, and $J - K$ photometric selections are 279, 257, and 252, respectively, demonstrating that the most influential criteria are the astrometric and $Z - K$ selections. Indeed, the additional $Y - J$ and $J - K$ selection remove small numbers of cluster member candidates. We stress that these cuts were chosen to recover known spectroscopic members from earlier surveys (see Section 3). These photometric selections returned 252 candidates in the region free of extinction (filled black dots in Fig. 4) and 396 in the region affected by reddening (filled black dots in Fig. 5). Similarly, we identified 84 member candidates in the SV region of the GCS.

We tested the influence of the choice of our selection lines on the final numbers of candidates, in the specific case of the $ZYJHK-PM$ sample without extinction. We shifted each selection line to the left and to the right by 0.1 mag, which corresponds roughly to the error on the colour (i.e. 1σ) at the faint end of the sequence at $J = 18$ mag. This shift corresponds to 2.5σ at $J = 17$ mag. We found that the shift to the blue of the six selection lines enumerated above yields roughly 20–30% more cluster member candidates. Similarly, a shift to the red gives about 20% less candidates in the $(Z - K, Z)$ diagram and 41–43% less in the other two diagrams.

We know that the level of contamination will be high in the region affected by reddening. Hence, we applied an additional photometric criterion in the $(Z - K, J - K)$ two-colour diagram (Fig. 6) to remove giants and reddened stars based on the location of previously-known spectroscopic members (red open squares; Lodieu et al. 2011). We selected sources satisfying the criteria:

- $(J - K) \geq 1.0$ for $(Z - K)$ between 1.7 and 2.4
- Sources below the line defined by $(Z - K, J - K) = (2.4, 1.0)$ and $(4.4, 1.85)$

This selection returned 201 and 120 sources (corresponding to 80% and 30% of the candidates left after the astrometric and the first three photometric selections) in the region with and without reddening, respectively. Only two candidates (or 2.5%) were rejected in the SV sample after applying this additional **criterion**. We list the coordinates, photometry, and proper motions of the candidates identified in $ZYJHK-PM$ (including known members published by other groups) in Tables A1 and B1 in the Appendix for the regions with and without reddening, respectively. We display their distribution in Fig. 1. We provide the list of member candidates within the SV area in Table C1.

We tested the influence of the choice of the crude selection in the $(Z - J, Z)$ colour-magnitude diagram by choosing a line **shifted** by 0.1 mag to the left of the original choice. We applied again the same aforementioned criteria and arrived at the same numbers of candidates for the two $ZYJHK-PM$ samples and the SV-only sample.

4.3 Catalogue summary

To summarise, we have identified a total of 688 sources in four different regions within USco: 195 and 111 in the $ZYJHK-PM$ regions without reddening and with extinction, 79 in the SV area, and 276 in the HK -only region. We found 11 sources in common among them, leaving 677 USco member candidates. We cross-matched this list with itself and found 4, 12, and 15 sources within 10, 50, and 100 arcsec of each other, pointing towards binary fractions for wide common proper motions of 0.6%, 1.8%, and 2.2% for projected separations of 1450 au, 7250 au, and 14500 au, respectively.

Table 3. Potential variable candidates in our USco $ZYJHK-PM$ sample of low-mass stars and brown dwarfs.

R.A.	dec	$K1$	$K2$	ΔK
15:52:33.93	-26:51:12.4	11.447	11.821	-0.374
16:23:23.06	-29:01:33.4	12.182	12.338	-0.156
15:47:22.82	-21:39:14.3	14.215	14.357	-0.142
16:23:22.02	-26:09:55.6	13.793	13.902	-0.109

5 VARIABILITY AT YOUNG AGES

We investigate the variability of low-mass stars and brown dwarfs in USco using the two K -band epochs provided by the GCS. Figure 7 shows the $(K1-K2)$ vs $K2$ diagram for USco member candidates in the $ZYJHK-PM$ sample. This analysis is not possible for the SV sample because no second K -band epoch is available.

The brightening in the $K1 = 10.5-11.5$ mag range is due to the difference in saturation between the first and second epoch, of the order of 0.5 mag both in the saturation and completeness limit. This is understandable because the exposure times have been doubled for the second epoch with relaxed constraints on the seeing requirement and weather conditions. We excluded those objects from our variability study. Overall, the sequence indicates consistent photometry between the two K epochs with very few objects being variable.

At first glance, we spotted four potential variables in Figure 7 (Table 3). The GCS images do not show anything anomalous so we did **not** proceed further. We selected variable objects by looking at the standard deviation, defined as $1.48 \times$ the median absolute deviation which is the median of the sorted set of absolute values of deviation from the central value of the $K1 - K2$ colour. We identified one potential variable object with a difference of 0.37 mag in the 11.5–12 mag range whereas the other three fainter candidates with differences between 0.1 and 0.16 mag lie just below the 3σ of the median absolute deviations of 0.05–0.06 mag. These small variations of the order of 0.1–0.15 mag can be interpreted by the presence of cool spots in low-mass stars (e.g. Scholz et al. 2009).

We conclude that the level of K -band variability at 5–10 Myr is small, with standard deviations of the order of 0.06 mag range, suggesting that it cannot account for the dispersion in the cluster sequence. We arrived at the same conclusions in the case of the Pleiades (Lodieu et al. 2012), α Per (Lodieu et al. 2012), and Praesepe (Boudreault et al. 2012) although these clusters are older (85, 120, and 590 Myr, respectively).

6 DISK FREQUENCY IN USCO

We cross-correlated our lists of candidates with the Wide Field Infrared Survey Explorer (WISE) All-sky release (Wright et al. 2010) using a matching radius of three arcsec. We found a total of 660 matches, divided into 194 in the $ZYJHK-PM$, 111 in the $ZYJHK-PM$ region with extinction, 79 objects in the SV-only area, and 276 counterparts in the HK -only region, respectively (Table E1). We looked at the WISE images and found that all WISE counterparts to the GCS objects are detected in $w1$ and $w2$. We classified the sources listed in Table E1 in two categories: 224 (33.9%) **source** detections in $w3$ but not in $w4$ and 58 (8.8%) objects detected in $w3$ and $w4$ marked as 1110 (open triangles in Figure 8) and 1111 (open squares in Figure 8), respectively. The

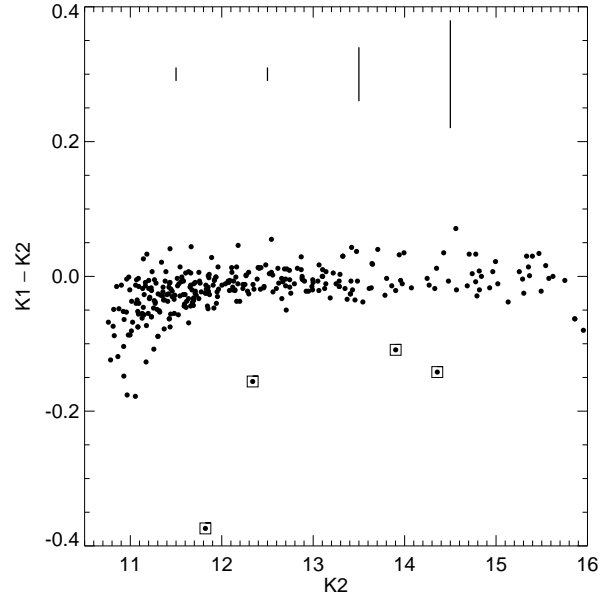


Figure 7. Difference in the K magnitude ($K1-K2$) as a function of the $K2$ magnitude for all USco member candidates with proper motions from GCS DR10. The four potential variable sources are highlighted with large open squares. Typical error bars on the colour shown as vertical dotted lines are added at the top of the plot.

latter objects detected in all WISE bands are unambiguous disk-bearing low-mass stars and brown dwarfs.

We considered two different methods to estimate the disk frequency of USco members with masses below $0.2 M_{\odot}$, according to the BT-Settl models (Allard et al. 2012). We plot in Figure 8 the $(w1 - w2, K)$ and $(K - w1, w1 - w3)$ diagrams. The former represents a good discriminant to separate disk-less and disk-bearing objects according to Dawson et al. (2012). We note that we chose K as the infrared band rather than J as in Dawson et al. (2012) because all targets in our four samples have K -band photometry. This diagram is efficient in Taurus but may not be the best criterion for USco where many transition disks are found (Riaz et al. 2012). The $(K - w1, w1 - w3)$ colour-colour diagram, however, clearly separates brown dwarf and M dwarf disks (Peña Ramírez et al. 2012) as well as primordial disks in USco (Figure 5 of Riaz et al. 2012).

We observe three sequences in the $(w1 - w2, K)$ diagram (left-hand side panel of Figure 8): one sequence to the left likely made of non-members mainly from the $ZYJHK-PM$ region with extinction and the HK -only area where our contamination is expected to be higher than in the other two areas ($ZYJHK-PM$ without reddening and SV-only). Optical spectroscopy is needed to confirm our claims though. Broadly, we have the same number of sources with disks (16% or 107 sources with $w1 - w2 \geq 0.4$ mag) as potential contaminants (100 sources or 15% with $w1 - w2 \leq 0.1$ mag), implying that the frequency of disk-bearing USco members lies between $107/600 = 16.2\%$ and $107/(660-100) = 19.1\%$, following the arguments of Dawson et al. (2012). However, these numbers are lower limits because 17/58 (29.3%) $w3 + w4$ detections have $w1 + w2$ colours bluer than 0.4 mag i.e. lie in the middle sequence, yielding corrected disk fractions of 18.8 and 22.1%. We are certainly missing some disk-bearing members hiding among $w3$ detections but it is harder to quantify without a cautious fitting of the spectral energy distributions (beyond the scope of this paper), as discussed

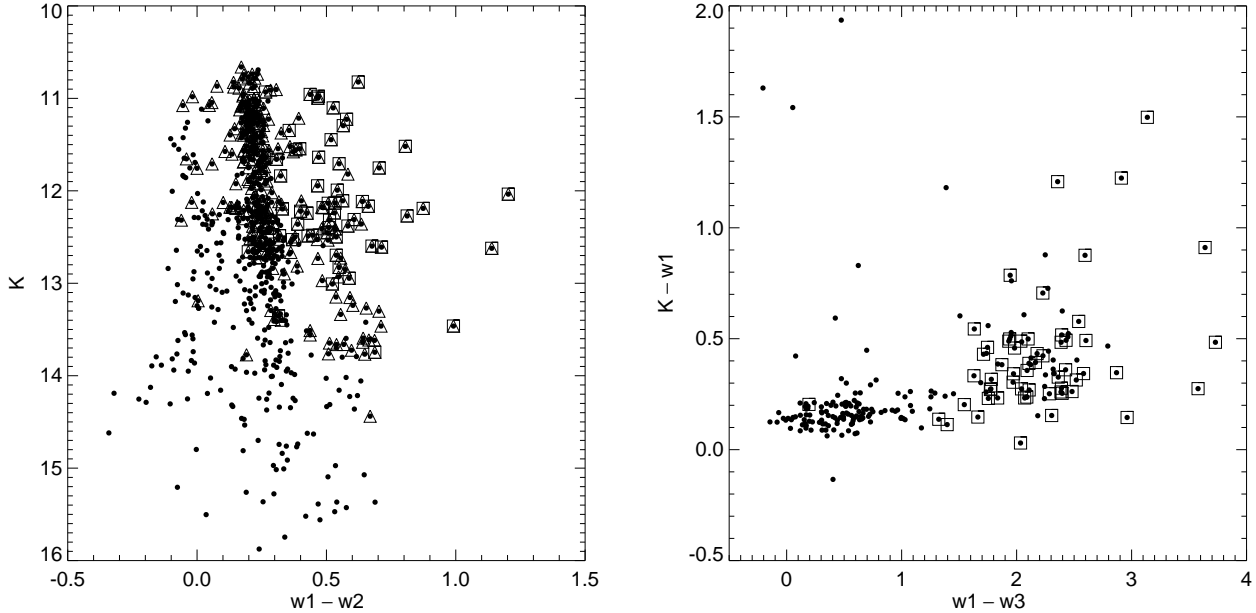


Figure 8. ($w1 - w2, K$) and ($w1 - w3, K - w1$) diagrams for USco members with WISE counterparts (black dots). Open triangles and open squares are sources detected in $w3$ and $w3 + w4$, respectively.

in details in Riaz et al. (2009) and Dawson et al. (2012). Nonetheless, we can place an upper limit of $(224+58)/660 = 42.7\%$ on the overall disk fraction for USco low-mass stars and brown dwarfs. Similarly, we can set a lower limit of $6/58 = 10\%$ based on the six unambiguous disk objects with $w1 + w2 \geq 0.8$ among sources detected in all four WISE bands.

We observe two groups of objects in the ($K - w1, w1 - w3$) diagram (right-hand side panel of Figure 8) depicting photospheric sources ($w1 - w3 \leq 1.2$ mag) and disk-bearing members ($w1 - w3 \geq 1.5$ mag). Objects in the middle may be good candidates to transition disks (Riaz et al. 2012). Among the 282 USco member candidates detected in three or four WISE bands, we have 89 sources with $w1 - w3 \geq 1.5$ mag, implying a disk fraction of 31.5% (most likely range of 26.6–37.1%). This fraction would increase by 5% if we include the potential transition disks.

The disk frequencies derived by both methods are consistent within the error bars although the second one is on average higher. Our values should be compared with the $23 \pm 5\%$ of Dawson et al. (2012) for USco brown dwarfs and $25 \pm 3\%$ of Luhman & Mamajek (2012) for M4–L2 members. For earlier-type members the disk **fractions** range from 10% for K0–M0 dwarfs (Luhman & Mamajek 2012) to 19% for K0–M5 dwarfs (Carpenter et al. 2006). Our disk fraction for USco substellar members is consistent with the $42 \pm 12\%$ and $36 \pm 8\%$ disk frequencies for brown dwarfs in IC 348 (1–3 Myr; Luhman et al. 2005) and σ Orionis (1–8 Myr; Peña Ramírez et al. 2012).

7 THE INITIAL MASS FUNCTION

We derive the cluster luminosity and system mass functions from our astrometric and photometric sample of ~ 320 USco member candidates distributed over ~ 50 square degrees (the *ZYJHK*–PM sample). We did not attempt to correct the mass function for binaries for two reasons. First, the presence of disks

around USco low-mass stars and brown dwarfs tend to displace these sources to the right-hand side of the sequence, implying that disentangling binaries from disk-bearing members is harder than in the case of more mature clusters like the Pleiades (Lodieu et al. 2012) and Praesepe (Boudeault et al. 2012). Second, a recent high-resolution imaging survey of 20 USco spectroscopic members fainter than $J = 15$ mag by Biller et al. (2011) resolved only one binary, pointing towards a binary frequency lower than 10%. This fraction is lower than the uncertainty on the number of sources per mass bin at the low-mass end, assuming Gehrels error bars.

7.1 The age of USco

de Zeeuw & Brand (1985) and de Geus et al. (1989) derived an age of 5–6 Myr comparing sets of photometric data with theoretical isochrones available at that time. Later, Preibisch & Zinnecker (1999) confirmed that USco is likely 5 Myr-old with a small dispersion on the age by placing about 100 spectroscopic members on the Hertzsprung–Russel diagram. This age estimate was later supported by Slesnick et al. (2008) from a wide-field optical study of low-mass stars and brown dwarfs with spectroscopic membership: these authors derived a mean age of 5 Myr with an uncertainty of 3 Myr taking into account all possible sources of uncertainties. More recently, Pecaut et al. (2012) argued for an age older (11 ± 2 Myr) from an analysis of the F-type members of the full Scorpius–Centaurus association. They determined older ages for all three subgroups forming Scorpius–Centaurus, including ages of 16 and 17 Myr for Upper Centaurus–Lupus and Lower Centaurus–Crux, which are older than the ages derived by Song et al. (2012) from the abundances of lithium in the spectra of F/K members of the association.

In this work, we adopt an age of 5 Myr for USco but we will also investigate the influence of age on the shape of the mass function (Section 7.3).

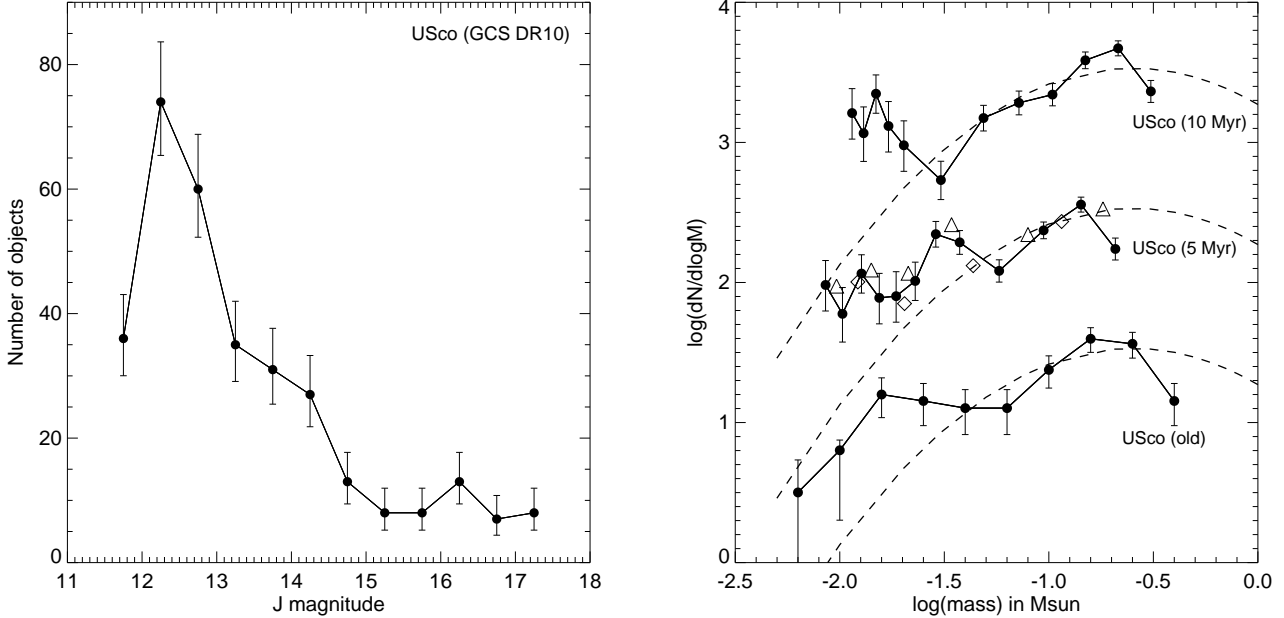


Figure 9. Luminosity (left) and mass (right) functions derived from our $ZYJHK-PM$ sample of USco member candidates. We plot the mass function for 5 and 10 Myr, ages quoted in the literature for USco as well as the mass function derived from the spectroscopic sample of Lodieu et al. (2011). Overplotted as a dashed line is the log-normal field mass function (Chabrier 2005). The binned mass functions are shown as open triangles (six bins) and open diamonds (four bins).

7.2 The cluster luminosity function

We construct the cluster luminosity function from our astrometric and photometric $ZYJHK-PM$ sample of 320 candidate members spanning $J = 11-17.5$ mag. We display the luminosity function divided into bins of 0.5 mag in the left panel of Fig. 9 with Gehrels error bars (Gehrels 1986). We note that the first and last bins are lower limits because of incompleteness at the bright and faint ends. We observe that the number of objects **decreases** with fainter magnitudes i.e. cooler temperatures.

7.3 The cluster mass function

We adopt the logarithmic form of the Initial Mass Function as originally proposed by Salpeter (1955): $\xi(\log_{10} m) = dn/d\log_{10}(m) \propto m^{-\alpha}$. We converted the luminosity into a mass using the BT-Settl models (Allard et al. 2012) and the J -band filter for all sources. We assumed a distance of 145 pc (van Leeuwen 2009) and an age of 5 Myr for USco (Table 4). We also considered an age of 10 Myr to compute the mass function (Table 5), keeping the same magnitude bins as a starting point.

We compare in Fig. 9 the mass function derived from our $ZYJHK-PM$ sample with the previous sample of spectroscopic members presented in Lodieu et al. (2011). We emphasise that the first and last bins are incomplete because of saturation on the bright side and incompleteness on the faint side. Both mass functions were computed assuming an age of 5 Myr but the earlier determination made use of the NextGen (Baraffe et al. 1998) and DUSTY (Chabrier et al. 2000) whereas we use the BT-Settl (Allard et al. 2012) with the new dataset presented here. Nonetheless, we observe that both mass functions are similar, with a possible excess of brown dwarfs below $\sim 0.03 M_{\odot}$ as originally claimed by Preibisch et al. (2001) and Slesnick et al. (2008). This excess of

substellar objects is enhanced if we consider an age of 10 Myr although it may be the result of the mass-luminosity relation, which does not reproduce the M7/M8 gap proposed by Dobbie et al. (2002) occurring around $0.015-0.02 M_{\odot}$ in USco (left panel in Fig. 9). Masses of brown dwarfs at 10 Myr are higher than at 5 Myr, making the number of substellar objects piling up at higher masses, causing an enhanced bump in the mass function. We computed the mass function using ages of 3 Myr and 1 Myr and found that the excess of brown dwarfs seems to disappear only if the association is 1 Myr, which is lower than any age estimate from previous studies. We observe that the high-mass part ($>0.03 M_{\odot}$) of the USco mass function is well reproduced by the log-normal form of the field mass function (Chabrier 2003, 2005), independently of the age chosen for USco (see Section 7.1).

We investigated the role of the bin size on the shape of the mass function, assuming an age of 5 Myr and a distance of 145 pc. We considered two options: on the one hand, we binned the mass function by a factor of two i.e. six bins instead of 12 (open triangles in Fig. 9), and, on the other hand, we employed four bins (open diamonds in Fig. 9) after removing the first and last bins which are incomplete (Table 4). We conclude that, overall, the bin size does not affect the shape of the mass function and the possible presence of the excess of low-mass brown dwarfs.

7.4 Comparison with other clusters

Figure 10 compares the USco mass function with our studies of the Pleiades (red open triangles; Lodieu et al. 2012) and σ Orionis (blue open squares; Lodieu et al. 2009). We note that the USco mass function is derived using the latest BT-Settl models (Allard et al. 2012) where former studies of the Pleiades and σ Orionis employed the NextGen (Baraffe et al. 1998) and DUSTY (Chabrier et al. 2000) models. The mass function of the Pleiades

Table 4. Values for the luminosity and mass functions for USco for an age of 5 Myr. We assumed a distance of 145 pc and employed the BT-Settl theoretical isochrones to transform magnitudes into masses (Allard et al. 2012). The mass function is plotted in Fig. 9.

Mag range	Nb_obj	Mass range	Mid-mass	dN	errH	errL	dlogM	errH	errL	dN/dM	errH	errL
11.5–12.0	36	0.2470–0.1690	0.2080	36.00	7.06	5.98	461.54	90.54	76.66	2.34	0.18	0.18
12.0–12.5	74	0.1690–0.1160	0.1425	74.00	9.65	8.59	1396.23	182.00	162.03	2.66	0.12	0.12
12.5–13.0	60	0.1160–0.0728	0.0944	60.00	8.79	7.73	1388.89	203.57	178.93	2.47	0.14	0.14
13.0–13.5	35	0.0728–0.0429	0.0578	35.00	6.98	5.89	1170.57	233.42	197.15	2.18	0.18	0.18
13.5–14.0	31	0.0429–0.0320	0.0374	31.00	6.63	5.55	2844.04	608.69	508.74	2.39	0.19	0.20
14.0–14.5	27	0.0320–0.0256	0.0288	27.00	6.27	5.17	4218.75	979.35	808.13	2.45	0.21	0.21
14.5–15.0	13	0.0256–0.0203	0.0230	13.00	4.71	3.57	2452.83	888.32	673.72	2.11	0.31	0.32
15.0–15.5	8	0.0203–0.0169	0.0186	8.00	3.96	2.78	2352.94	1164.13	818.79	2.00	0.40	0.43
15.5–16.0	8	0.0169–0.0140	0.0155	8.00	3.96	2.78	2758.62	1364.84	959.96	1.99	0.40	0.43
16.0–16.5	13	0.0140–0.0114	0.0127	13.00	4.71	3.57	5000.00	1810.81	1373.35	2.16	0.31	0.32
16.5–17.0	7	0.0114–0.0092	0.0103	7.00	3.78	2.60	3181.82	1719.95	1180.94	1.88	0.43	0.46
17.0–17.5	8	0.0092–0.0079	0.0086	8.00	3.96	2.78	6153.85	3044.65	2141.45	2.08	0.40	0.43

Table 5. Values for the luminosity and mass functions for USco for an age of 10 Myr. We assumed a distance of 145 pc and employed the BT-Settl theoretical isochrones to transform magnitudes into masses (Allard et al. 2012). The mass function is plotted in Fig. 9.

Mag range	Nb_obj	Mass range	Mid-mass	dN	errH	errL	dlogM	errH	errL	dN/dM	errH	errL
11.5–12.0	36	0.3620–0.2530	0.3075	36.00	7.06	5.98	330.28	64.79	54.85	2.36	0.18	0.18
12.0–12.5	74	0.2530–0.1760	0.2145	74.00	9.65	8.59	961.04	125.27	111.53	2.67	0.12	0.12
12.5–13.0	60	0.1760–0.1230	0.1495	60.00	8.79	7.73	1132.08	165.93	145.85	2.59	0.14	0.14
13.0–13.5	35	0.1230–0.0852	0.1041	35.00	6.98	5.89	925.93	184.63	155.95	2.34	0.18	0.18
13.5–14.0	31	0.0852–0.0587	0.0720	31.00	6.63	5.55	1169.81	250.37	209.26	2.28	0.19	0.20
14.0–14.5	27	0.0587–0.0387	0.0487	27.00	6.27	5.17	1350.00	313.39	258.60	2.17	0.21	0.21
14.5–15.0	13	0.0387–0.0222	0.0305	13.00	4.71	3.57	787.88	285.34	216.41	1.73	0.31	0.32
15.0–15.5	8	0.0222–0.0183	0.0203	8.00	3.96	2.78	2051.28	1014.88	713.82	1.98	0.40	0.43
15.5–16.0	8	0.0183–0.0159	0.0171	8.00	3.96	2.78	3333.33	1649.18	1159.95	2.12	0.40	0.43
16.0–16.5	13	0.0159–0.0139	0.0149	13.00	4.71	3.57	6500.00	2354.05	1785.36	2.35	0.31	0.32
16.5–17.0	7	0.0139–0.0121	0.0130	7.00	3.78	2.60	3888.89	2102.16	1443.38	2.07	0.43	0.46
17.0–17.5	8	0.0121–0.0108	0.0115	8.00	3.96	2.78	6153.85	3044.65	2141.45	2.21	0.40	0.43

comes from a photometric and astrometric selection using GCS DR9 in the same manner as this work in USco. Both mass functions are very comparable in the interval where they overlap, from $\sim 0.2 M_{\odot}$ down to $\sim 0.03 M_{\odot}$ and match the log-normal form of the field mass function (Chabrier 2005). We note that the Pleiades mass function is comparable to the mass functions in α Per (Lodieu et al. 2012) and Praesepe (Boudreault et al. 2012) using the same GCS DR9 database in a homogeneous manner. This result is in line with the numerous mass functions plotted in Figure 3 of Bastian et al. (2010), demonstrating the similarities between mass functions in many clusters over a broad range of masses.

We plot in Figure 10 the mass function for the young (1–8 Myr) σ Ori cluster derived from a pure photometric study using the fourth data release of the GCS (blue open squares; Lodieu et al. 2009). The shape of the σ Ori mass function agrees with the field mass function in the $0.2\text{--}0.01 M_{\odot}$ mass range, as noted by independent studies of the cluster (Béjar et al. 2001; Caballero et al. 2007; Bihain et al. 2009; Béjar et al. 2011; Peña Ramírez et al. 2012).

8 SUMMARY

We have presented the outcome of a deep and wide photometric and proper motion survey in the USco association as part of the UKIDSS GCS DR10. The main results of our analysis are:

- we recovered several hundred known USco members and up-

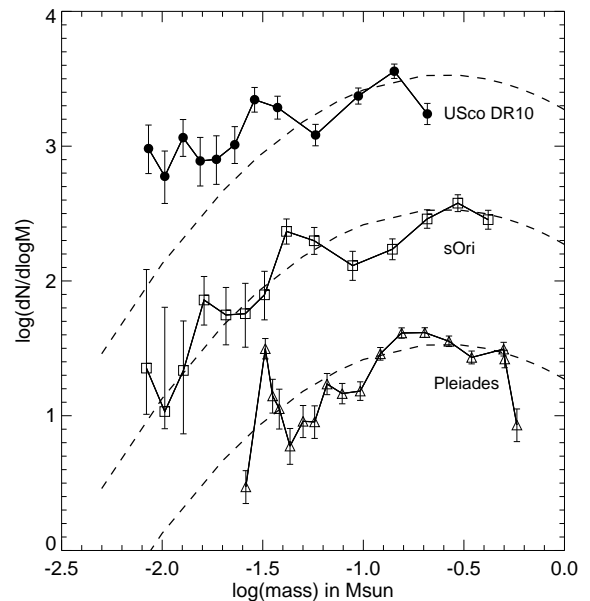


Figure 10. Mass function of USco derived from our GCS DR10 sample compared to the Pleiades (red open triangles; Lodieu et al. 2012) and σ Orionis (blue open squares; Lodieu et al. 2009). Overplotted as a black dashed line is the log-normal field mass function (Chabrier 2005).

dated their membership with the proper motion and photometry available from GCS DR10.

- we selected photometrically and astrometrically new potential USco member candidates and identified about 700 candidates within regions free of extinction and regions affected by reddening.
- we derived the luminosity function in the USco association in the $J = 11.5\text{--}17.5$ mag range.
- we derived the USco mass function which matches well the log-normal form of the system field mass function down to $0.03 M_{\odot}$. The USco mass function is consistent with the Pleiades, α Per, and Praesepe mass functions in the $0.2\text{--}0.03 M_{\odot}$ mass range. We observe a possible excess of substellar members below $0.03 M_{\odot}$, as pointed out by earlier studies (Preibisch et al. 2001; Lodieu et al. 2007; Slesnick et al. 2008), which may be due to the uncertainties on the mass-luminosity relation at the M/L transition and the age of the association.

This paper provides a full catalogue of photometric and astrometric members from $0.2 M_{\odot}$ down to $\sim 0.01 M_{\odot}$ in the southern part of the USco association. This catalogue is complemented by a complete census of the stellar and substellar populations in full association USco down to $0.02\text{--}0.015 M_{\odot}$. This work will represent a reference for many years to come. We foresee further improvement when a second epoch will be obtained for the northern part of the association as part of the VISTA hemisphere survey (Emerson et al. 2004; Dalton et al. 2006). Our study provides a legacy sample that can be used to study the disk properties of low-mass stars and brown dwarfs in USco (Carpenter et al. 2006; Scholz et al. 2007; Riaz et al. 2009; Dawson et al. 2012; Luhman & Mamajek 2012), their binary properties (Biller et al. 2011), and their distribution in the association as a function of spectral type once a complete spectroscopic follow-up is available.

ACKNOWLEDGMENTS

NL is funded by the Ramón y Cajal fellowship number 08-303-01-02 and the national program AYA2010-19136 funded by the Spanish ministry of science and innovation. **I thank the anonymous referee for her/his constructive and quick report.** This work is based in part on data obtained as part of the UKIRT Infrared Deep Sky Survey (UKIDSS). The UKIDSS project is defined in Lawrence et al. (2007). UKIDSS uses the UKIRT Wide Field Camera (WFCAM; Casali et al. 2007). The photometric system is described in Hewett et al. (2006), and the calibration is described in Hodgkin et al. (2009). The pipeline processing and science archive are described in Irwin et al. (2004) and Hambly et al. (2008), respectively. We thank our colleagues at the UK Astronomy Technology Centre, the Joint Astronomy Centre in Hawaii, the Cambridge Astronomical Survey and Edinburgh Wide Field Astronomy Units for building and operating WFCAM and its associated data flow system. We are grateful to France Allard for placing her latest BT-Settl models on a free webpage for the community.

This research has made use of the Simbad database, operated at the Centre de Données Astronomiques de Strasbourg (CDS), and of NASA's Astrophysics Data System Bibliographic Services (ADS).

This publication makes use of data products from the Two Micron All Sky Survey (2MASS), which is a joint project of the University of Massachusetts and the Infrared Processing and Analysis Center/California Institute of Technology, funded by the National Aeronautics and Space Administration and the National Science Foundation.

REFERENCES

- Allard F., Homeier D., Freytag B., 2012, Royal Society of London Philosophical Transactions Series A, 370, 2765
- Ardila D., Martín E., Basri G., 2000, AJ, 120, 479
- Baraffe I., Chabrier G., Allard F., Hauschildt P. H., 1998, A&A, 337, 403
- Bastian N., Covey K. R., Meyer M. R., 2010, ARA&A, 48, 339
- Béjar V. J. S., et al. 2001, ApJ, 556, 830
- Béjar V. J. S., Zapatero Osorio M. R., Rebolo R., Caballero J. A., Barrado D., Martín E. L., Mundt R., Bailer-Jones C. A. L., 2011, ApJ, 743, 64
- Bihain G., et al. 2009, A&A, 506, 1169
- Biller B., Allers K., Liu M., Close L. M., Dupuy T., 2011, ApJ, 730, 39
- Boudreault S., Lodieu N., Deacon N. R., Hambly N. C., 2012, MNRAS, 426, 3419
- Caballero J. A., et al. 2007, A&A, 470, 903
- Carpenter J. M., Mamajek E. E., Hillenbrand L. A., Meyer M. R., 2006, ApJL, 651, L49
- Casali M., et al. 2007, A&A, 467, 777
- Chabrier G., 2003, PASP, 115, 763
- Chabrier G., 2005, in E. Corbelli, F. Palla, & H. Zinnecker ed., The Initial Mass Function 50 Years Later Vol. 327 of Astrophysics and Space Science Library, The Initial Mass Function: from Salpeter 1955 to 2005. p. 41
- Chabrier G., Baraffe I., Allard F., Hauschildt P., 2000, ApJ, 542, 464
- Collins R., Hambly N., 2012, in "Ballester P., Egret D., eds, Astronomical Data Analysis Software and Systems XXI Vol. in press, of Astronomical Society of the Pacific Conference Series, Calculating proper motions in the WFCAM Science Archive for the UKIRT Infrared Deep Sky Surveys
- Dalton G. B., et al. 2006, in Society of Photo-Optical Instrumentation Engineers (SPIE) Conference Series Vol. 6269 of Presented at the Society of Photo-Optical Instrumentation Engineers (SPIE) Conference, The VISTA infrared camera
- Dawson P., Scholz A., Ray T. P., 2011, A&A
- Dawson P., Scholz A., Ray T. P., Marsh K. A., Wood K., Natta A., Padgett D., Ressler M. E., 2012, MNRAS
- de Bruijne J. H. J., Hoogerwerf R., Brown A. G. A., Aguilar L. A., de Zeeuw P. T., 1997, in ESA SP-402: Hipparcos - Venice '97 Improved Methods for Identifying Moving Groups. pp 575–578
- de Geus E. J., de Zeeuw P. T., Lub J., 1989, A&A, 216, 44
- de Zeeuw P. T., Hoogerwerf R., de Bruijne J. H. J., Brown A. G. A., Blaauw A., 1999, AJ, 117, 354
- de Zeeuw T., Brand J., 1985, in Boland W., van Woerden H., eds, Birth and Evolution of Massive Stars and Stellar Groups Vol. 120 of Astrophysics and Space Science Library, Photometric age determination of OB-association. pp 95–101
- Dobbie P. D., Pinfield D. J., Jameson R. F., Hodgkin S. T., 2002, MNRAS, 335, L79
- Emerson J. P., Sutherland W. J., McPherson A. M., Craig S. C., Dalton G. B., Ward A. K., 2004, The Messenger, 117, 27
- Gehrels N., 1986, ApJ, 303, 336
- Hambly N. C., et al. 2008, MNRAS, 384, 637
- Hewett P. C., Warren S. J., Leggett S. K., Hodgkin S. T., 2006, MNRAS, 367, 454
- Hodgkin S. T., Irwin M. J., Hewett P. C., Warren S. J., 2009, MNRAS, 394, 675
- Irwin M. J., et al. 2004, eds, Optimizing Scientific Return for Astronomy through Information Technologies. Edited by Quinn,

- Peter J.; Bridger, Alan. Proceedings of the SPIE, Volume 5493, pp. 411-422 (2004). VISTA data flow system: pipeline processing for WFCAM and VISTA. pp 411-422
- Kroupa P., 2002, *Science*, 295, 82
- Kroupa P., Weidner C., Pflamm-Altenburg J., Thies I., Dabringhausen J., Marks M., Maschberger T., 2011, ArXiv e-prints
- Kunkel M., 1999, Ph.D. Thesis, Julius-Maximilians-Universität Würzburg
- Lawrence A., Warren S. J., Almaini O., Edge A. C., Hambly N. C., 17 co-authors 2007, *MNRAS*, 379, 1599
- Lodieu N., Deacon N. R., Hambly N. C., 2012, *MNRAS*, p. 2699
- Lodieu N., Deacon N. R., Hambly N. C., Boudreault S., 2012, *MNRAS*, 426, 3403
- Lodieu N., Dobbie P. D., Hambly N. C., 2011, *A&A*, 527, A24
- Lodieu N., Hambly N. C., Dobbie P. D., Cross N. J. G., Christensen L., Martín E. L., Valdivielso L., 2011, *MNRAS*, 418, 2604
- Lodieu N., Hambly N. C., Jameson R. F., 2006, *MNRAS*, 373, 95
- Lodieu N., Hambly N. C., Jameson R. F., Hodgkin S. T., 2008, *MNRAS*, 383, 1385
- Lodieu N., Hambly N. C., Jameson R. F., Hodgkin S. T., Carraro G., Kendall T. R., 2007, *MNRAS*, 374, 372
- Lodieu N., Zapatero Osorio M. R., Rebolo R., Martín E. L., Hambly N. C., 2009, *A&A*, 505, 1115
- Luhman K. L., et al. 2005, *ApJL*, 631, L69
- Luhman K. L., Mamajek E. E., 2012, *ApJ*, 758, 31
- Martín E. L., Delfosse X., Guieu S., 2004, *AJ*, 127, 449
- Martín E. L., et al. 2010, *A&A*, 517, A53
- Miller G. E., Scalo J. M., 1979, *ApJS*, 41, 513
- Peña Ramírez K., Béjar V. J. S., Zapatero Osorio M. R., Petrotzens M. G., Martín E. L., 2012, *ApJ*, 754, 30
- Pecaut M. J., Mamajek E. E., Bubar E. J., 2012, *ApJ*, 746, 154
- Preibisch T., Guenther E., Zinnecker H., 2001, *AJ*, 121, 1040
- Preibisch T., Guenther E., Zinnecker H., Sterzik M., Frink S., Roeser S., 1998, *A&A*, 333, 619
- Preibisch T., Zinnecker H., 1999, *AJ*, 117, 2381
- Preibisch T., Zinnecker H., 2002, *AJ*, 123, 1613
- Riaz B., Lodieu N., Gizis J. E., 2009, *ApJ*, 705, 1173
- Riaz B., Lodieu N., Goodwin S., Stamatellos D., Thompson M., 2012, *MNRAS*, 420, 2497
- Salpeter E. E., 1955, *ApJ*, 121, 161
- Scalo J. M., 1986, *Fundamentals of Cosmic Physics*, 11, 1
- Scholz A., Jayawardhana R., Wood K., Meeus G., Stelzer B., Walker C., O’Sullivan M., 2007, *ApJ*, 660, 1517
- Scholz A., Xu X., Jayawardhana R., Wood K., Eislöffel J., Quinn C., 2009, *MNRAS*, 398, 873
- Slesnick C. L., Carpenter J. M., Hillenbrand L. A., 2006, *AJ*, 131, 3016
- Slesnick C. L., Hillenbrand L. A., Carpenter J. M., 2008, *ApJ*, 688, 377
- Song I., Zuckerman B., Bessell M. S., 2012, *AJ*, 144, 8
- van Leeuwen F., 2009, *A&A*, 497, 209
- Walter F. M., Vrba F. J., Mathieu R. D., Brown A., Myers P. C., 1994, *AJ*, 107, 692
- Wright E. L., et al. 2010, *AJ*, 140, 1868

APPENDIX A: USCO MEMBER CANDIDATES IN THE ZYJHK-PM REGION FREE OF REDDENING

APPENDIX B: USCO MEMBER CANDIDATES IN THE ZYJHK-PM REGION AFFECTED BY REDDENING

APPENDIX C: USCO MEMBER CANDIDATES IN THE GCS SV

APPENDIX D: USCO MEMBER CANDIDATES IN THE HK SAMPLE

APPENDIX E: USCO MEMBER CANDIDATES WITH WISE PHOTOMETRY

Table A1. Sample of 201 USco member candidates in the GCS DR10 PM region devoid of reddening, including known members previously published in the literature. This table is available electronically in the online version of the journal.

R.A.	Dec.	$Z \pm \text{err}$	$Y \pm \text{err}$	$J \pm \text{err}$	$H \pm \text{err}$	$K1 \pm \text{err}$	$K2 \pm \text{err}$	$\mu_{\alpha \cos \delta} \pm \text{err}$	$\mu_{\delta} \pm \text{err}$	χ^2
15:41:26.54	-26:13:25.5	15.649±0.005	14.788±0.003	13.999±0.003	13.406±0.003	12.971±0.002	12.986±0.002	-7.31±2.70	-17.66±2.70	0.58
15:41:54.34	-25:12:43.6	15.588±0.005	99.999±99.999	14.435±0.004	13.729±0.003	13.422±0.003	13.457±0.003	-8.05±1.97	-24.10±1.97	4.28
...
16:37:05.23	-26:25:44.2	14.266±0.003	13.605±0.002	12.963±0.002	12.461±0.002	12.082±0.001	12.088±0.001	-7.65±2.69	-20.81±2.69	0.68
16:37:54.43	-26:51:52.0	12.968±0.001	12.507±0.001	11.923±0.001	11.459±0.001	11.096±0.001	11.142±0.001	-6.53±2.69	-22.52±2.69	0.84

Table B1. Sample of 120 USco member candidates in the GCS DR10 PM region affected by reddening, including known members previously published in the literature. This table is available electronically in the online version of the journal.

R.A.	Dec.	$Z \pm \text{err}$	$Y \pm \text{err}$	$J \pm \text{err}$	$H \pm \text{err}$	$K1 \pm \text{err}$	$K2 \pm \text{err}$	$\mu_{\alpha \cos \delta} \pm \text{err}$	$\mu_{\delta} \pm \text{err}$	χ^2
16:16:20.73	-25:17:30.1	13.316±0.002	12.800±0.001	12.192±0.001	11.528±0.001	11.171±0.001	11.231±0.001	-4.56±1.82	-16.57±1.82	0.53
16:16:30.68	-25:12:20.3	14.208±0.003	13.549±0.002	12.887±0.001	12.320±0.002	11.935±0.001	11.936±0.001	-12.30±1.82	-19.96±1.82	0.48
...
16:39:49.31	-24:33:10.1	14.232±0.003	13.771±0.002	13.169±0.002	12.501±0.001	12.267±0.001	12.266±0.001	-12.25±1.83	-21.05±1.83	0.54
16:40:47.51	-24:04:38.9	19.594±0.069	18.269±0.030	17.073±0.022	15.881±0.014	15.364±0.015	15.334±0.010	-7.17±2.38	-17.62±2.38	8.88

Table C1. Sample of 81 USco member candidates identified in the GCS SV area, including previously-known members. The proper motion measurements come from the 2MASS/GCS cross-match. This table is available electronically in the online version of the journal.

R.A.	Dec.	$Z \pm \text{err}$	$Y \pm \text{err}$	$J \pm \text{err}$	$H \pm \text{err}$	$K1 \pm \text{err}$	$\mu_{\alpha \cos \delta}$	μ_{δ}
16:06:03.75	-22:19:30.0	18.169±0.036	16.825±0.014	15.853±0.009	15.096±0.009	14.438±0.009	13.67	-26.51
16:06:06.29	-23:35:13.3	18.430±0.041	17.150±0.018	16.204±0.012	15.540±0.012	14.973±0.012	-6.08	5.64
...
16:17:01.47	-23:29:06.0	13.656±0.002	13.025±0.002	12.453±0.001	11.887±0.001	11.537±0.001	-17.93	-19.58
16:17:06.06	-22:25:41.6	13.254±0.002	12.663±0.002	12.120±0.001	11.516±0.001	11.202±0.001	-15.03	-26.36

Table D1. Sample of 286 USco member candidates identified in the USco region imaged in H and K only, including previously-known members. This table is available electronically in the online version of the journal.

R.A.	Dec.	$H \pm \text{err}$	$K \pm \text{err}$	$\mu_{\alpha \cos \delta}$	μ_{δ}
15:40:10.22	-24:31:18.4	14.538±0.004	13.818±0.004	0.31	-9.96
15:41:16.03	-25:30:56.5	14.932±0.008	14.305±0.008	-9.04	-7.19
...
16:40:19.60	-22:18:12.0	13.361±0.002	12.953±0.002	0.36	-5.89
16:40:24.95	-22:18:52.8	12.871±0.002	12.450±0.002	5.38	-13.56

Table E1. Sample of 660 USco member candidates identified in GCS DR10 with WISE photometry, ordered by increasing right ascension. The coordinates are from the UKIDSS GCS DR10 database whereas the photometry is from the WISE all-sky release. Objects detected in two, three, and four WISE bands are marked as 1100, 1110, and 1111 (column 7; wise_detect), respectively. This table is available electronically in the online version of the journal.

R.A.	Dec.	$w1 \pm \text{err}$	$w2 \pm \text{err}$	$w3 \pm \text{err}$	$w4 \pm \text{err}$	wise_detect
15:40:10.22	-24:31:18.4	13.733±0.031	13.829±0.048	12.462±0.000	8.811±0.000	1100
15:41:16.03	-25:30:56.5	14.226±0.034	14.330±0.079	12.185±0.000	8.764±0.000	1100
...
16:40:24.95	-22:18:52.8	12.113±0.024	12.012±0.028	11.473±0.278	7.397±0.117	1100
16:40:47.51	-24:04:38.9	15.028±0.054	14.773±0.093	11.426±0.000	8.249±0.000	1100